4328–4334 *Nucleic Acids Research, 1999, Vol. 27, No. 22*

A theoretical approach to select effective antisense oligodeoxyribonucleotides at high statistical probability

Volker Patzel, Ulrich Steidl[1], Ralf Kronenwett[1], Rainer Haas[1,2] and Georg Sczakiel*

Forschungsschwerpunkt Angewandte Tumorvirologie and [1]Klinische Kooperationseinheit Molekulare Hämatologie/Onkologie, Deutsches Krebsforschungszentrum, Im Neuenheimer Feld 242, D-69120 Heidelberg, Germany and [2]Medizinische Klinik und Poliklinik V, Universität Heidelberg, D-69115 Heidelberg, Germany

Received August 27, 1999; Revised and Accepted September 27, 1999

ABSTRACT

Up to now, out of approximately 20 antisense oligodeoxyribonucleotides (asODN) selected and tested against a given target gene, only one species shows substantial suppression of target gene expression. In part, this seems to be related to the general assumption that the structures of local target sequences or antisense nucleic acids are unfavorable for efficient annealing. Experimental approaches to find effective asODN are extremely expensive when including a large number of antisense species and when considering their moderate success. Here, we make use of a systematic alignment of computer-predicted secondary structures of local sequence stretches of the target RNA and of semi-empirical rules to identify favorable local target sequences and, hence, to design more effective asODN. The intercellular adhesion molecule 1 (*ICAM-1*) gene was chosen as a target because it had been shown earlier to be sensitive to antisense-mediated gene suppression. By applying the protocol described here, 10 *ICAM-1*-directed asODN species were found that showed substantially improved inhibition of target gene expression in the endothelial cell line ECV304 when compared with the most effective published asODN. Further, 17 out of 34 antisense species (50%) selected on the theoretical basis described here showed significant (>50%) inhibition of *ICAM-1* expression in mammalian cells.

INTRODUCTION

Antisense nucleic acids have become a major tool to study gene function in developmental biology and assist in genome exploration projects, to suppress malignant or aberrant gene expression in molecular medicine, and to produce higher value products in commercial terms in plant molecular biology. Besides the elementary biological question whether a given gene of interest is suitable for a successful antisense approach to inhibit its expression, a major current task is to select efficient antisense species out of the complex sequence space of antisense nucleic acids that is defined by the target sequence. A number of approaches to identify promising long chain or oligomeric antisense nucleic acids are based on experimental strategies. For long chain artificial antisense RNA, annealing kinetics *in vitro* (1,2) and global flexibility (2) seem to be related to efficacy in living cells. Both properties are strongly dependent on secondary and tertiary structures of the complementary strands. Conversely, short antisense oligonucleotides, particularly oligodeoxyribonucleotides (ODN), have a restricted ability to form stable intramolecular structures. Their efficacy may be related to thermodynamic as well as kinetic parameters mainly determined by the local target sequences and their adopted structures (3,4). Published work suggests that only one out of 18–20 tested oligonucleotides shows significant inhibition of target gene expression (5,6). Possible rules for the annealing of complementary nucleic acids are complex and not widely understood. For example, the extension or shortening of a given antisense sequence by as few as 1 or 2 nt may crucially alter annealing efficiency *in vitro* (1,3,7) and efficacy in living cells (1). Experimental procedures have been developed to select efficient antisense oligonucleotide species out of the space of all possible oligomeric antisense sequences with significant success (3,4,8). These methods are mainly based on annealing reactions with arrays of antisense species (3) or monitoring accessibility of target structures by RNase H mapping (4,9). Such experimental procedures and their success, however, are affected by experimental limitations which cannot be excluded or even controlled sufficiently. For example, a complete and equal representation of antisense species in the starting pool of selection procedures is hard to achieve. Further, different oligonucleotide species tested in a mixture may positively interfere with each other, i.e. they may provide a 'facilitator function' for annealing with the target RNA, which has been reported in specific cases (10,11). Similarly, interference may be negative, i.e. efficiently annealing antisense species may not be recognized when tested in a mixture. Such limitations inherent to complex experimental procedures can be abolished, in principle, if computational procedures are used to generate and to analyse the complete antisense sequence space against a given target sequence. Most theoretical

*To whom correspondence should be addressed. Tel: +49 6221 424939; Fax: +49 6221 424932; Email: sczakiel@dkfz-heidelberg.de
Present addresses:
Ralf Kronenwett and Rainer Haas, Universität Düsseldorf, Klinik für Hämatologie, Onkologie und Klinische Immunologie, Moorenstraße 5, D-40225 Düsseldorf, Germany

approaches described so far are based on parameters of low resolution such as the 'local folding potential' (12) or on individual secondary structure predictions of the target RNA and/or thermodynamic duplex stabilities (13,14). However, none of these theoretical approaches has been able to substitute for experimental work so far.

Here, a computer-aided and semi-empirical procedure is presented to systematically and substantially increase the statistical probability of selecting effective antisense oligonucleotide species out of the space of all possible oligomeric antisense sequences. To test this procedure experimentally we used the gene encoding intercellular adhesion molecule 1 (*ICAM-1*), which plays an important role in inflammatory diseases (15–17). Published data convincingly describe antisense-specific and effective inhibition of *ICAM-1* by antisense oligonucleotides in tissue culture (18,19), in rodents (20,21), and in humans (22), indicating that *ICAM-1* represents a cellular target gene that is well suited to gene suppression by antisense ODN (asODN). This is reflected in ongoing clinical phase IIb studies with *ICAM-1*-directed asODN (22). Thus, the published effective *ICAM-1*-directed asODN provide valid and powerful positive controls for efficacy in this study (18,19) which is important to validate the usefulness of the new theoretical approach described here to select effective antisense species.

Although the *ICAM-1* gene has been studied extensively with respect to effective antisense inhibitors, the theoretical approach described here revealed 17 asODN that suppressed *ICAM-1* to similar or higher levels than the so far most effective asODN species (18). Ten of these selected antisense sequences showed significant (>50%) and up to 3-fold stronger inhibition of *ICAM-1* in endothelial ECV304 cells when compared with the most potent species described in the literature so far. The findings of this work seem to be of general rather than *ICAM-1*-specific importance and could be helpful in searching for effective antisense oligonucleotides against any given target sequence.

MATERIALS AND METHODS

Oligodeoxyribonucleotides

All oligonucleotides were purchased from commercial suppliers. They were synthesized as phosphorothioate derivatives and purified by HPLC.

Computer programs

To predict secondary structures of asODN, we used the software Oligo v.3.4, which is based on the work of Breslauer *et al*. (23). The program mfold 2.0 is included in the Heidelberg Unix Sequence Analysis Resources (HUSAR) (24).

Cell lines and cell culture

The endothelial cell line ECV304 (ATCC, Manassas, VA), derived from spontaneously transformed human umbilical vein endothelial cells (25), was cultured in medium 199 (Life Technologies, Karlsruhe, Germany) supplemented with 10% FCS, L-glutamine (2 mmol/l), penicillin (100 IU/ml) and streptomycin (100 μg/ml) and passaged twice a week after trypsinization. For stimulation of endothelial cells 200 U/ml interleukin 1β (IL-1β) (PromoCell, Heidelberg, Germany) were added to the medium 16 h before analysis of *ICAM-1* expression.

Treatment of cells with ODN

ECV304 cells were treated with ODN as described (18). In brief, cells were grown to between 60 and 80% confluency in 6-well culture plates and washed with prewarmed (37°C) serum-free Opti-MEM medium (Life Technologies). Aliquots of 500 μl of Opti-MEM containing 5 μg/ml of the cationic lipid DOTMA/DOPE (Lipofectin; Life Technologies) were added to the cells followed by the addition of 500 μl Opti-MEM containing the ODN (final concentration 0.1 μM). The cells were incubated for 4 h at 37°C. Subsequently, the transfection medium was replaced by medium 199 containing 10% FCS. After an incubation of 4 h at 37°C the medium was again substituted with medium 199 containing 10% FCS and 200 U/ml IL-1β to stimulate *ICAM-1* expression. For immunofluorescence analysis endothelial cells were removed from the culture plate by trypsinization for 5 min with 1 ml, trypsin/EDTA at 37°C 16 h after stimulation with IL-1β. This short trypsinization did not significantly influence the surface expression of *ICAM-1* in comparison with cells harvested with a cell scraper.

Immunofluorescence staining and flow cytometry

After washing with phosphate-buffered saline (PBS), 1×10^5 cells were incubated with a phycoerythrin (PE)-conjugated *ICAM-1* /CD54-PE monoclonol antibody (clone LB-2; Becton Dickinson, Heidelberg, Germany) or an isotype-identical control (Becton Dickinson) in 500 ml PBS containing 1% BSA at 4°C for 30 min. Following antibody staining, cells were washed and suspended in PBS buffer. The cells were analysed using a Becton Dickinson FACScan and CELL QUEST software (Becton Dickinson, Heidelberg, Germany). The mean fluorescence intensity was used to calculate the percentage inhibition in comparison to control expression using the formula: {[(*ICAM-1* expression of ODN-treated cytokine-stimulated cells) – (basal *ICAM-1* expression)]/[(*ICAM-1* expression of cytokine-stimulated cells) – (basal *ICAM-1* expression)]} × 100.

RESULTS

Computational identification of favorable local target sites

The annealing of long chain complementary RNA is strongly influenced by the structures of both strands and experimental evidence suggests that specific secondary structure elements of antisense RNA are crucial for the effectiveness of duplex formation and efficacy in living cells (2,26,27). These include sequence stretches that are not involved in intramolecular hydrogen bonding and are not part of rigid structural elements, such as for example extra stable tetraloops (28). Here, we assume that the annealing of short chain antisense oligonucleotides with long chain target RNA is, in structural terms, mainly influenced by local target structures whereas the effects of possible structures of the ODN are negligible. From earlier studies we determined that favorable local target structures include stem–loop elements in which the loop size extends a certain minimal size of ~10 nt, bulges of similar size, joint sequences connecting individual folding units (7), and terminal sequences that are not involved in intramolecular interactions (29). Based on these considerations, a computer algorithm was generated to predict secondary structures (mfold 2.0) of a set of subsequences (windows) of a given target RNA and to record positions of the target sequence for which favorable structure

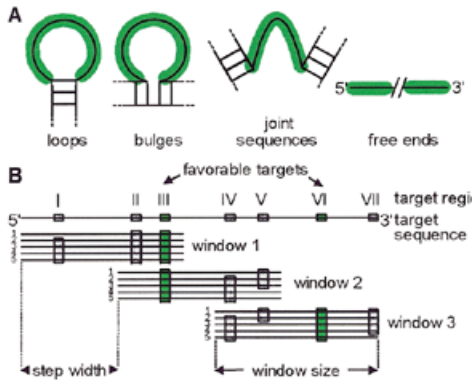

Figure 1. Schematic depiction of the computer-aided selection of favorable local target elements. (**A**) Secondary structure motifs that are assumed to contain accessible sequences (green) and, thus, are favorable targets for antisense ODN include large loops, bulges, joints and free ends. (**B**) Local targets are selected if favorable structural elements are conserved among a set of minimum free energy structures and among all shifted windows (indicated by green boxes).

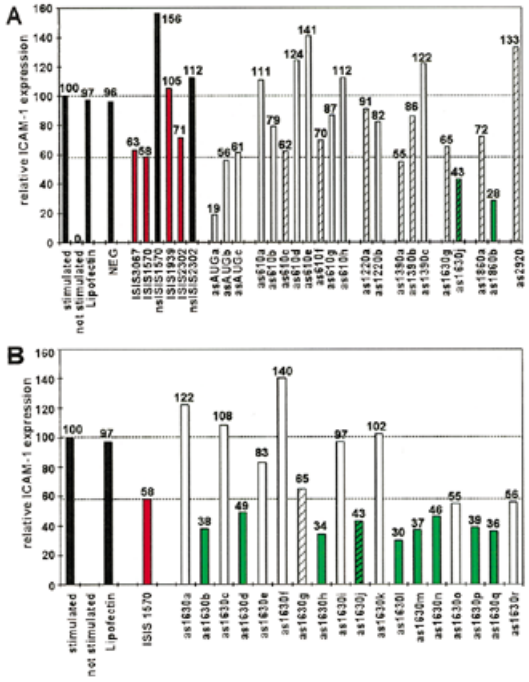

Figure 2. Inhibition of *ICAM-1* expression in ECV304 cells by transfected asODN. Efficacy of asODN directed against a set of six local targets (**A**) and efficacy of asODN against the local target region t1630 (**B**). Effective published asODN are represented by red bars, black bars indicate controls, hatched bars (white or green) indicate effects of asODN identified in the first round of theoretical selection, and all open bars indicate effects of asODN identified in the second round of theoretical selection. Selected asODN with substantially improved inhibition of *ICAM-1* expression compared to the most effective published asODN are represented by green bars.

elements occured (Fig. 1). A window of 1400 nt was used in this work and was shifted along the target sequence at a step width of 250 nt. Such predicted potentially favorable local structures, according to the above listed favorable motifs, were compared between different overlapping sequence stretches and the five lowest energy structures (mfold 2.0) for each window (Fig. 1). Antisense ODN sequences were chosen if potentially favorable local structure elements occured in all predicted structures of overlapping sequence stretches and in all lowest energy structures.

The theoretical analysis of the *ICAM-1* mRNA (30) suggested six promising local target sequences including sequences around positions 610, 1220, 1390, 1630, 1860 and 2920, according to the numbering by Tomassini *et al.* (31). Three of these local targets (t610, t1390 and t1630) were thought to have a higher probability of being favorable since they were more conserved among the secondary structure predictions.

Inhibition of *ICAM-1* gene expression by selected asODN

Next, we tested experimentally whether theoretically selected asODN species were related to increased frequency of significant inhibition of target gene expression. Antisense ODN sequences were chosen such that their 3′- or 5′-end was not directed against intramolecularly folded target sequences.

Expression of *ICAM-1* was induced in ECV304 cells by IL-1β 8 h after Lipofectin-mediated transfection of oligonucleotides. Expression levels of *ICAM-1* were determined by flow cytometry following staining with an ICAM-1-directed monoclonal antibody. This test system had been used before to measure inhibition of *ICAM-1* gene expression by a set of four effective published antisense species, including ISIS2302 and ISIS1570 (18,19). In a first round, a set of nine antisense 20mers directed against all six local targets of the *ICAM-1* mRNA (Fig. 2A, hatched bars) was tested in human endothelial ECV304 tissue culture cells according to a standard protocol (18). The results show that four of the six predicted target regions, t610, t1390, t1630 and t1860, seemed to be accessible to the selected asODN (Fig. 2A). Strongest inhibition of 57% occured with the asODN as1630j and the extent of inhibition was even stronger than that of the so far most effective sequences described, ISIS1570, ISIS1939, ISIS2302 and ISIS3067 (18,19), ranging between 0 and 42% in this study. No inhibition was observed with the asODN termed NEG in Figure 2A, which was directed against a target site that was predicted to be unfavorable according to the above algorithm. It served here as a negative control.

Subsequently, a larger number of asODN against five of the six local target regions were tested (Fig. 2). This included a set of overlapping species against target region t1630 (Fig. 2B) and three antisense species covering the AUG start codon (Fig. 2A). Antisense species against the targets tAUG (asAUGa), t1630 (as1630b, as1630h, as1630l, as1630m, as1630p and as1630q), and t1860 (as1860b) showed strongest inhibition of *ICAM-1*, ranging between 61 and 81% under the experimental conditions used here. In total, out of 34 asODN selected according to the computational approach and tested in this work, 17 (50%) suppressed *ICAM-1* gene expression significantly (>50%; see Fig. 2). Ten antisense species (29%; green bars in Fig. 2) showed up to a 3-fold increased extent of inhibition when compared with the, so far, most effective

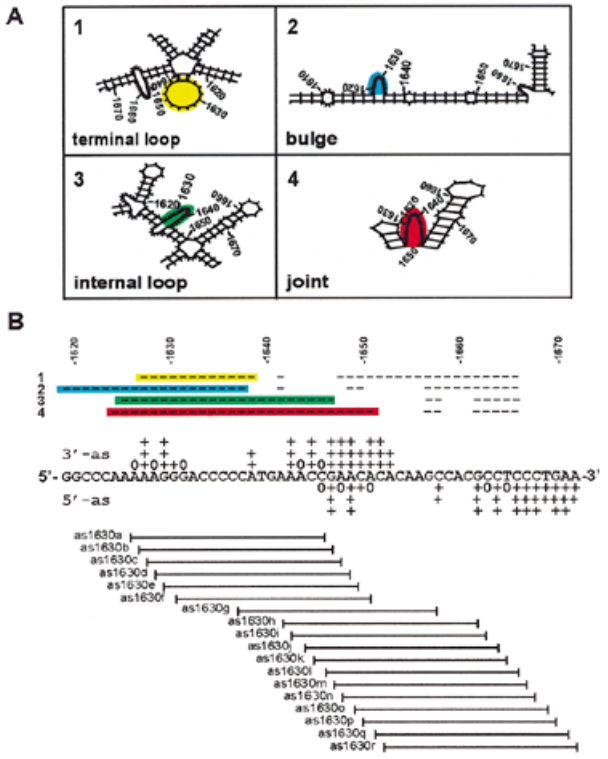

Figure 3. Structure–function relationship of asODN against the local target t1630. Either of four alternative favorable local target structures occurs in all secondary structure predictions for t1630 (**A**) and relationship between the location of 3′- and 5′-ends of effective t1630-directed asODN, the accessibility of alternatively predicted local target structures, and efficacy against expression of *ICAM-1* in cell culture (**B**). Unpaired nucleotides occuring in local target structures 1–4 (A) are indicated by – and color coded according to the coloring in (A). The target sequence (30) is shown 5′→3′ (numbering according to Tomassini *et al*.; 31). The position of 3′-termini (above target sequence) and 5′- ends of t1630-directed asODN (below target sequence) and their efficacy are indicated: 0, no significant inhibition (<10%); +, weak inhibition (10–25%); ++, inhibition comparable to asODN that served as positive controls (26–50%); +++, inhibition of asODN stronger than positive controls (>50%).

published *ICAM-1*-directed antisense oligonucleotides (18,19) (Fig. 2, red bars).

Structure–function relationship

The set of overlapping antisense species against the target t1630 (Fig. 2B) allows one, in principle, to look at higher resolution at the relationship between local target structures and efficacy in living cells. Four different local target structures of t1630 sequences occured in all predictions depending on the chosen window and when considering other low energy structures beside the lowest energy structure. The secondary structures predicted to be adopted by the t1630 region included a terminal loop, two different internal loops (bulges), and a joint (Fig. 3A). Among the group of t1630-directed overlapping asODN, some species had no measurable effect on *ICAM-1* expression (e.g. as1630a, as1630c, as1630f, as1630i and as1630k) whereas other species (e.g. as1630l, as1630h and as1630q) were among the strongest inhibitors (Fig. 2B). The transition from strong to weak inhibition was sharp for antisense species such as, for example, as1630h, as1630i, as1630j, as1630k and as1630l. This means that the shift of the sequence of an effective antisense 20mer by 1 nt along the target sequence led to complete loss of inhibition and *vice versa* which is related to the change of one complementary nucleotide at either terminus of the asODN (Figs 2B and 3B). These base exchanges do not significantly alter the base composition nor the thermodynamic DNA/RNA duplex stability and the findings are consistent with the view that free 3′- and 5′-ends, regardless of their base composition, are important for efficacy and, presumably, annealing of asODN in living cells.

DISCUSSION

In order to obtain insights into the relationship between target structure and efficacy we considered a number of properties that had been shown to be relevant or that seemed relevant to us. These include: (i) the possible role of terminal nucleotides for the initiation of annealing; (ii) specific sequence motifs of the antisense and target sequences, respectively; (iii) sequence motifs that had been shown or postulated to play a role for efficacy; and (iv) the possible biological function of the local target sequences. A summary of these parameters and their relation to efficacy in ECV304 cells is shown in Table 1.

This work provides information on the relationship between primary selected sequences and efficacy of asODN-mediated gene silencing in mammalian cells. Besides specific structural properties of local target sequences that seem to favor efficacy, like the motifs shown in Figure 3A, however, there is no obvious link between primary sequence and efficacy in cultured cells via biological or biochemical parameters. This is important to note because, in contrast to recent attempts to improve the design of asODN on the basis of mechanistic assumptions, this work shows a way to directly relate nucleotide sequences to efficacy. The algorithm used here is based on conventional RNA structure predictions with varying overlapping sequence stretches and a set of different low energy structures, thereby increasing the statistical probability of looking at relevant structures. This might help to overcome the weakness of RNA secondary structure prediction with individual sequences. One might hypothesize that the frequency at which a given sequence stretch occurs within favorably predicted local structures (see Fig. 1) is related to the probability of designing effective asODN. On the other hand, this means that only a small portion of potentially favorable target sites identified by single target structure predictions are promising candidates for antisense targets which might explain the lack of correlation between individual target structure predictions and experimental scanning procedures (4,9,32).

The positive results described here, however, seem to be suited to shed some light on structural and mechanistic aspects: stretches of 10 or more consecutive nucleotides of the target RNA which are not involved in intramolecular base pairing seem to be suitable target regions that are long enough to allow efficient annealing with asODN at specific sites. The low frequency at which large joints, bulges, or loops occur in secondary structure predictions is not surprising when considering that 5.5 nt is the average loop size of stem–loops on a statistical basis (33). Favorable target sites predicted in different windows and different low energy structures occur at a low

Table 1. Relationship between characteristics of the sequences of *ICAM-1*-directed asODN and their efficacy in human ECV304 cells

Name	Target position	Inhibition	Target region[a]	G+C	Terminal bases		Possible initiation[b]	Pyrimidines		Target GGGA	Self-complementarity[c]	ODN dimer formation[d]
					5′-end	3′-end		Total	Contiguous			
ISIS3067	32–51	++	5′-UTR	11	TC	CT		8	3	No	3–4 bp	Yes
ISIS1570	64–81	++	AUG	12	TG	CG		6	2	No	3 bp	Yes
ISIS1939	1952–1971	0	3′-UTR	14	CC	CT		18	10	Yes	≤2 bp	No
ISIS2302	2114–2133	++	3′-UTR	13	GC	AC		11	3	No	3 bp	Yes
NEG	1364–1383	0	cds	9	GG	AG		9	5	No	3–4 bp	Yes
asAUGa	59–78	+++	AUG	13	GA	GG		6	2	No	3–4 bp	Yes
asAUGb	61–80	++	AUG	13	GG	AG		7	2	No	3–4 bp	Yes
asAUGc	63–82	++	AUG	13	CT	TC		8	2	No	3–4 bp	Yes
as610a	593–612	0	cds	11	CA	CC	5′	14	9	No	3–5 bp	Yes
as610b	598–617	+	cds	12	GG	CC	5′	13	7	No	≤2 bp	Yes
as610c	603–622	++	cds	9	AA	CT	Middle	10	4	No	≤2 bp	Yes
as610d	607–626	0	cds	10	CG	TG	3′	9	4	No	3 bp	Yes
as610e	609–628	0	cds	10	CA	GT	3′	9	4	No	3 bp	Yes
as610f	610–629	++	cds	10	GC	TA	3′	9	4	No	3 bp	Yes
as610g	611–630	+	cds	11	GG	AG	3′	8	4	No	3 bp	Yes
as610h	615–634	0	cds	12	GT	CG	3′	7	2	No	3 bp	Yes
as1220a	1219–1238	0	cds	12	CT	TG	3′	14	5	Yes	≤2 bp	Yes
as1220b	1223–1242	+	cds	13	GA	CT	3′	11	5	Yes	3 bp	Yes
as1390a	1384–1403	++	cds	12	TG	GT	Middle	10	6	Yes	3 bp	Yes
as1390b	1390–1409	+	cds	11	AG	GG	3′	11	6	Yes	≤2 bp	Yes
as1390c	1391–1410	0	cds	11	CA	GT	3′	12	6	Yes	3 bp	Yes
as1630a	1626–1645	0	cds	11	GG	TT	3′ or 5′	12	7	Yes	≤2 bp	Yes
as1630b	1627–1646	+++	cds	12	CG	TT	3′ or 5′	12	6	Yes	≤2 bp	Yes
as1630c	1628–1647	0	cds	12	TC	TC	3′ or 5′	12	5	Yes	≤2 bp	Yes
as1630d	1629–1648	+++	cds	12	TT	CC	3′ or 5′	12	4	Yes	≤2 bp	Yes
as1630e	1630–1649	+	cds	12	GT	CC	3′ or 5′	11	4	No	≤2 bp	Yes
as1630f	1631–1650	0	cds	11	TG	CT	3′ or 5′	11	4	No	≤2 bp	Yes
as1630g	1638–1657	++	cds	9	GC	TA	3′	13	4	No	≤2 bp	No
as1630h	1642–1661	+++	cds	11	CG	TT	3′	12	3	No	≤2 bp	No
as1630i	1643–1662	0	cds	12	GC	TG	3′	11	3	No	≤2 bp	No
as1630j	1644–1663	+++	cds	13	GG	GG	3′	10	3	No	≤2 bp	No
as1630k	1645–1664	0	cds	12	AG	GC	3′	10	3	No	≤2 bp	No
as1630l	1646–1665	+++	cds	12	GA	CT	3′	10	3	No	≤2 bp	No
as1630m	1647–1666	+++	cds	12	GG	TT	3′	9	3	No	≤2 bp	No
as1630n	1648–1667	+++	cds	13	GG	TG	3′	8	3	No	≤2 bp	No
as1630o	1649–1668	++	stop	13	AG	GT	3′	7	3	No	≤2 bp	No
as1630p	1650–1669	+++	stop	13	CA	TG	3′	8	3	No	≤2 bp	No
as1630q	1651–1670	+++	stop	13	TC	GT	3′	8	3	No	≤2 bp	No
as1630r	1652–1671	++	stop	12	TT	TG	3′	9	3	No	≤2 bp	No
as1860a	1851–1870	++	3′-UTR	10	GA	TT	3′	11	4	No	≤2 bp	Yes
as1860b	1855–1874	+++	3′-UTR	11	AT	GT	3′	9	3	No	≤2 bp	Yes
as2920	2914–2933	0	3′-UTR	2	TG	CT	Middle	3	2	No	≤2 bp	No

[a]5′-UTR, 5′-untranslated region; 3′-UTR, 3′-untranslated region; AUG, start codon AUG; cds, coding sequences; stop, translational stop codon.
[b]Possible initiation of duplex formation via the respective portion of the asODN.
[c]Number of consecutive intramolecular base pairs according to the program Oligo v.3.4.
[d]Dimer formation according to the program Oligo v.3.4.

frequency of approximately one site per 1000 nt (data not shown). We favor the idea that initiation of duplex formation is critical and, as observed here, this seems to occur especially via the free 3′-end of the antisense strand (Table 1). This view is supported by the summary shown in Figure 3B: it is the 3′-end of effective antisense species (e.g. as1630h, as1630j, as1630l, as1630m, as1630n, as1630p and as1630q) which is complementary to favorable target sequences and not their 5′-end, which becomes particularly obvious if one considers the joint as the potential target motif (Fig. 3A, structures 4). Further, when regarding target nt 1647 and 1650, as1630m and as1630p with their 3′-ends directed against these positions are among the strongest inhibitors whereas as1630c and as1630f with their 5′-ends directed against the same nucleotides do not show any measurable effect (Fig. 3B). These findings are consistent with a number of reports on derivatives of antisense RNA with a constant 5′-end and successively elongated 3′-ends which indicate that annealing, stability and efficacy may be strongly influenced by single nucleotides (1,3).

Regarding the biological role of the local target sequences, this work indicates a preference for the AUG start codon as a local target (tAUG). All tAUG-directed asODN were effective, including the potent inhibitor asAUGa, but were not selected according to theoretical structure prediction. It is important to note that this theoretical approach would not have been able to predict these tAUG-directed antisense species. One might speculate that asODN directed against the start codon or upstream sequences may suppress apparent gene expression by a mechanism that is different from the usually assumed pathway via RNase H activity. For example, the vicinity of the target AUG could be temporarily accessible and well suited for duplex formation such that the ordered assembly of ribosomal components might be blocked by AUG-directed asODN. However, beside the AUG start codon, strong antisense inhibitors may be directed against some but not all parts of the coding sequence (see Table 1, columns 3 and 4), against the stop codon as well as against the 3′-untranslated region (UTR) (e.g. as1860b). Published data on the use of ISIS3067 also show that the 5′-UTR may serve as a favorable target (19). The importance of target accessibility to antisense strands is further supported by the lack of efficacy of asODN NEG, which was directed against a conserved intramolecularly base paired target stretch.

It seems reasonable to assume that the annealing of asODN and target RNA in living cells critically involves free 3′- or 5′-ends of the antisense strands because, on a statistical basis, terminal bases are less affected by steric hindrance and volume exclusion effects. Thus, ends have a higher probability of being accessible to intermolecular interactions than internal sequences. Further, terminal nucleotides are, statistically, more flexible than central ones, which favors nucleation of double strand formation. The lack of correlation between motifs at the level of primary structure and efficacy (Table 1, columns 5, 6 and 8) indicates that crucial steps of asODN-mediated suppression of *ICAM-1* gene expression are not directly related to the primary sequence. Here, primary sequences determined predicted secondary structures. These served as the crucial basis for the theoretical approach described here, which was successful on a statistical level. However, even secondary structure prediction of the local target (Fig. 3) cannot explain the variable inhibitory potential of the overlapping t1630-directed antisense sequences, suggesting that the highly sequence-specific effects might be due to highly varying individual properties, i.e. accessibility for initiation of annealing of single bases within the three-dimensional target structure.

Regarding the role of target sequences and terminal nucleotides of asODN, the simplest model would assume that efficient pairing preferentially requires nucleotides that are not involved in intramolecular interactions. This is the case for joint sequences and terminal unpaired sequences as well as for external or internal loops, empirically estimated to be larger than ~10 nt. However, neither 5′-located nor 3′-positioned dinucleotides of effective asODN show a preference for stable Watson–Crick base pairing, i.e. show a preference for G-C base pairs (Table 1, column 6), although in most cases, target sequences are predicted to be accessible to termini of antisense species (Table 1, column 7). The inhibition data of the set of t1630-directed asODN were related to alternatively predicted models for the local secondary structure of this target (Fig. 3A) and favor the stem–loop (isoform 1 in Fig. 3A) or the joint (isoform 4 in Fig. 3A) since only for these target structures can one of the two termini of the effective antisense species meet its complementary target at accessible sites. Empirically, we favor the joint as being the relevant target structure because external sequence units, such as free ends and joint sequences rather than free bases in bulges or loops, seem to favor efficient annealing of complementary nucleic acids and efficacy on a statistical basis (2,26).

This study does not indicate any relationship between the thermodynamic stability of the DNA/RNA duplex formed between antisense and target sequences which is reflected in the GC content and the extent of inhibition (Table 1, columns 3 and 5). Even when considering specific primary sequence motifs, no obvious relationship occurs. For example, Ratmeyer *et al*. suggested that stretches of ribopurines within the target can stabilize DNA–RNA heteroduplexes (34). Thus, one might conclude that such sequences support annealing as well as efficacy of asODN. The set of *ICAM-1*-directed antisense species tested here, however, does not indicate that contiguous purines in the target RNA are related to efficacy (Table 1, column 8). Further, Tu *et al*. showed that a GGGA motif occurs in the target RNA at a statistically higher frequency in the case of effective asODN and concluded that antisense species containing the complementary TCCC motif have a >50% probability of being effective in the case of sequences of tumor necrosis factor-α (35). The findings described in this work, however, do not support this view: the TCCC motif occurs in several effective as well as ineffective *ICAM-1*-directed antisense species. Finally, we looked at intramolecular folding of the asODN and the possibility of dimer formation, both of which, however, were not related to efficacy (Table 1, columns 10 and 11).

In this work we have described a theoretical approach that substantially increases the probability of successful selection of asODN that are effective in living cells. This approach is oriented towards the successful application of asODN and it is substantially less expensive than experimental strategies based on assumptions that are often not definitive and, thus, cannot guarantee success. This method might not neccessarily be able to identify antisense sequences with maximal efficacy without further experimental scanning or substantially improved insights into the rules governing the action of asODN at ‘single nucleotide resolution’. This work, however, might serve as a

platform to reach this mechanistic goal with realistic and moderate effort when compared to conventional experimental strategies and techniques because it bypasses experimental limitations and substantially reduces time and costs. This theoretical approach may clearly facilitate the search for and development of new antisense molecules of academic and commercial interest.

ACKNOWLEDGEMENTS

We thank K.-H. Glatting for computational help and the Deutsche Forschungsgemeinschaft for financial support. We also thank members of A3D GmbH–Antisense Design and Drug Development for helpful advice.

REFERENCES

1. Rittner,K., Burmester,C. and Sczakiel,G. (1993) *Nucleic Acids Res.*, **21**, 1381–1387.
2. Patzel,V. and Sczakiel,G. (1998) *Nature Biotechnol.*, **16**, 64–68.
3. Milner,N., Mir,K.U. and Southern,E.M. (1997) *Nature Biotechnol.*, **15**, 537–541.
4. Ho,S.P., Bao,Y., Lesher,T., Malhotra,R., Ma,L.Y., Fluharty,S.J. and Sakai,R.R. (1998) *Nature Biotechnol.*, **16**, 59–63.
5. Peyman,A., Helsberg,M., Kretzschmar,G., Mag,M., Grabley,S. and Uhlmann,E. (1995) *Biol. Chem. Hoppe-Seyler*, **367**, 195–198.
6. Monia,B.P., Johnston,J.F., Geiger,T., Muller,M. and Fabbro,D. (1996) *Nature Med.*, **2**, 668–675.
7. Patzel,V., zu Putlitz,J., Wieland,S., Blum,H.E. and Sczakiel,G. (1997) *Biol. Chem. Hoppe-Seyler*, **378**, 539–543.
8. Lima,W.F., Brown-Driver,V., Fox,M., Hanecak,R. and Bruice,T.W. (1997) *J. Biol. Chem.*, **272**, 626–638.
9. Scherr,M. and Rossi,J.J. (1998) *Nucleic Acids Res.*, **26**, 5079–5085.
10. Pachuk,C.J., Yoon,K., Moelling,K. and Coney,L.R. (1994) *Nucleic Acids Res.*, **22**, 301–307.
11. Jankowsky,E. and Schwenzer,B. (1996) *Biochemistry*, **35**, 15313–15321.
12. Sczakiel,G., Homann,M. and Rittner,K. (1993) *Antisense Res. Dev.*, **3**, 45–52.
13. Denman,R.B. (1993) *Biotechniques.*, **15**, 1090–1095.
14. James,W. and Cowe,E. (1997) *Methods Mol. Biol.*, **74**, 17–26.
15. Rothlein,R., Dustin,M.L., Marlin,S.D. and Springer,T.A. (1986) *J. Immunol.*, **137**, 1270–1274.
16. Griffiths,C.E., Voorhees,J.J. and Nickoloff,B.J. (1989) *J. Am. Acad. Dermatol.* **20**, 617–629.
17. Bernstein,C.N., Sargent,M. and Gallatin,W.M. (1998) *Clin. Immunol. Immunopathol.*, **86**, 147–160.
18. Chiang,M.-Y., Chan,H., Zounes,M.A., Freier,S.M., Lima,W.F. and Bennett,C.F. (1991) *J. Biol. Chem.*, **266**, 18162–18171.
19. Bennett,C.F., Condon,T.P., Grimm,S., Chan,H. and Chiang,M.Y. (1994) *J. Immunol.*, **152**, 3530–3540.
20. Stepkowski,S.M., Wang,M.E., Amante,A., Kalinin,D., Qu,X., Blasdel,T., Condon,T., Kahan,B.D. and Bennett,F.C. (1997) *Transplant. Proc.*, **29**, 1285.
21. Bennett,C.F., Kornbrust,D., Henry,S., Stecker,K., Howard,R., Cooper,S., Dutson,S., Hall,W. and Jacoby,H.I. (1997) *J. Pharmacol. Exp. Ther.*, **280**, 988–1000.
22. Yacyshyn,B.R., Bowen-Yacyshyn,M.B., Jewell,L., Tami,J.A., Bennett,C.F., Kisner,D.L. and Shanahan,W.R.,Jr (1998) *Gastroenterology*, **114**, 1133–1142.
23. Breslauer,K.J., Frank,R., Blocker,H. and Marky,L.A. (1986) *Proc. Natl Acad. Sci. USA*, **83**, 3746–3750.
24. Senger,M., Glatting,K.-H., Ritter,O. and Suhai,S. (1995) *Comput. Programs Biomed.*, **46**, 131–141.
25. Takahashi,K., Sawasaki,Y., Hata,J., Mukai,K. and Goto,T. (1990) *In Vitro Cell Dev. Biol.*, **26**, 265–274.
26. Eckardt,S., Romby,P. and Sczakiel,G. (1997) *Biochemistry*, **36**, 12711–12721.
27. Lima,W.F., Monia,B.P., Ecker,D.J. and Freier,S.M. (1992) *Biochemistry*, **31**, 12055–12061.
28. Uhlenbeck,O.C. (1990) *Nature*, **346**, 613–614.
29. Schwille,P., Oehlenschläger,F. and Walter,N.G. (1996) *Biochemistry*, **35**, 10182–10193.
30. Staunton,D.E., Marlin,S.D., Stratowa,C., Dustin,M.L. and Springer,T.A. (1988) EMBL accession no. HSICAM01.
31. Tomassini,J.E., Graham,D., DeWitt,C.M., Lineberger,D.W., Rodkey,J.A. and Colonno,R.J. (1989) *Proc. Natl Acad. Sci. USA*, **86**, 4907–4911.
32. Birikh,K.R., Berlin,Y.A., Soreq,H. and Eckstein,F. (1997) *RNA*, **3**, 429–437.
33. Fontana,W., Konings,D., Stadler,P.F. and Schuster,P. (1993) *Biopolymers*, **33**, 1389–1404.
34. Ratmeyer,L., Vinayak,R., Zhong,Y.Y., Zon,G. and Wilson,W.D. (1994) *Biochemistry*, **33**, 5298–5304.
35. Tu,G.C., Cao,Q.N., Zhou,F. and Israel,Y. (1998) *J. Biol. Chem.*, **273**, 25125–25131.